



High belite cement from alternative raw materials

H.Y. Ghorab^a✉, M. Rizk^a, B. Ibrahim^b, M.M. Allam^b

a. Helwan University (Cairo, Egypt)

b. Tourah Cement Company - Suez Cement Group, Cairo, Egypt (Cairo, Egypt)
✉ hanaa.ghorab@gmail.com

Received 13 March 2013

Accepted 9 October 2013

Available on line 23 May 2014

ABSTRACT: Three high belite laboratory clinkers were prepared from traditional and alternative raw materials. Reference clinker was obtained from 77% limestone, 11% sandy clays, 11% fatty clays and 1% iron scales. The fatty clays were replaced by red brick powder in the raw meal of the second clinker and were lowered to 2% with the replacement of 10% of the limestone by egg shells in the third clinker. The SEM examination revealed clear presence of crossed striae and twinning in the rounded belite grains of the reference clinker caused by the transformation of the α' -belite to the β polymorph. Striae were weaker in the second and third clinkers indicating a probable stabilization of the α' -belite polymorph.

Compressive strength of the respective cements were attained first after 28 days and the early strength did not improve with increasing fineness. Higher compressive strength values were found for the cement prepared from second clinker.

KEYWORDS: Clinker; α Belite; Stabilization; Alternative raw materials

Citation / Citar como: Ghorab, H.Y.; Rizk, M.; Ibrahim, B.; Allam, M.M. (2014) High belite cement from alternative raw materials *Mater. Construcc.* 64 [314], e012 <http://dx.doi.org/10.3989/mc.2014.01913>.

RESUMEN: *Cementos con altos contenidos en belita obtenido a partir de materias primas alternativas.* Se han preparado tres clinker de laboratorio con altos contenidos en belita a partir de materias primas tradicionales y alternativas. El clinker de referencia se obtuvo a partir de una mezcla de caliza, arcillas arenosas y grasas y limaduras de hierro. Las arcillas grasas fueron sustituidas por polvo de ladrillo rojo en la preparación del segundo clinker, y en el tercero el contenido de arcilla grasa fue de solo un 2% y parte de la caliza fue sustituida por cascara de huevo.

El estudio realizado por SEM muestra superficies estriadas alrededor de los granos de belita que indican una transformación del polimorfo α' a la forma β -C₂S, durante el enfriamiento. Esas estrías son menos marcadas en el segundo y tercer clinker, indicando, una estabilización del polimorfo α' -C₂S.

Los valores de resistencias a compresión de los correspondientes cementos, a 28 días de curado, no se ven incrementados por la finura de dichos cementos. Las mayores resistencias se obtuvieron en el cemento preparado a partir del clinker con polvo de ladrillo rojo.

PALABRAS CLAVE: Clinker; α' -Belita; Estabilización; Materias primas alternativas

Copyright: © 2014 CSIC. This is an open-access article distributed under the terms of the Creative Commons Attribution-Non Commercial (by-nc) Spain 3.0 License.

1. INTRODUCTION

Portland cement is an essential component for the daily life. It is one of the most consumed materials in the world. The global cement consumption

was expected to grow from 448 kg/person in 2009, to 539 kg/person in 2012 and to 645 kg/person by 2017 (1). The cement industry in the Arab world represents ~6% of the world production which amounts to ~3.3 Bt cement/year (2). 168 cement plants with a

production capacity of 235 Mt cement/year are presently found in this area and shall expand to ~310 Mt cement/year within the next five years. Oil and natural gas formulates 98% of the energy sources needed for the power plants; the cement industry alone consuming 2.1% of the primary fuel of the total industrial sector, with an energy cost of ~40–60% from the total production expenses (3).

On the other hand, the climate change is directly related to the CO₂ emission. On the global level, the cement industry produces ~1.4 Bt CO₂/year, i.e. ~6% of the total CO₂ production and ~4% of the global warming (4, 5). 54% from the CO₂ are provided from the calcination process, 34% from the fuel combustion and ~12% from the electricity. An average of 0.83 tons of CO₂ is emitted per ton of cement with 80% clinker (6).

There is therefore an urgent need to reduce the energy consumption and the CO₂ emission in the cement sector. Recent data revealed that a good utilization of waste materials might reduce the CO₂ emission by up to 9% (7).

One way to achieve these targets is to limit the consumption of Portland cement clinker by enhancing the production of blended cements within the scope of the international standard specifications such as EN 197-1, EN 14216 and ES 4756 (8–10). Most of the cement replacement materials cited in the specification are industrial wastes of suitable latent hydraulic properties. Several authors were concerned with the production of the low energy belite cements using wastes materials of environmental benefits, such as fly ash (11–14), rice hull ash (15) or slag (16).

Other solutions deal with the partial substitution of the high-lime cement by the lower temperature belite phase with the stabilization of the more active belite polymorph, the α' -phases (17, 18). Belite-type of cement also referred as “green” is of great economic and environmental interest. It reduces the CO₂ and the energy consumptions due to the lower firing temperature and the lower limestone content compared to alite cement. The energy demand is estimated to be 15–20% less than that needed for ordinary Portland cement at a lime saturation factor of 80–85% (19–20). A drop in the lime saturation standard of the kiln meal from 100 to 88% results in a reduction in fuel requirement from 3800 kJ/kg to 3400 KJ/kg in the energy – and raw materials dependent CO₂ emission by 10% (21).

To overcome the lack of early strength, the high belite cements are blended with calcium sulfoaluminate or sulfoferrite (22, 23). Belite cements with limited hydraulic reactivity are interesting for massive constructions thanks to their limited heat of hydration.

The activation of a low temperature clinker through the stabilization of the α' -belite modification adds value to the cement manufacture process and leads to better durability.

Another important aspect related to the reduction of the production costs is the use of alternative raw materials and/or alternative fuels (24–29). The extent of this subject is diverse and needs deeper understanding.

The aim of the present paper deals with the use of alternative raw materials to contribute to the reduction of energy, CO₂ and production cost. In this work, the effect of replacing parts of the clays and limestone with red brick powder and egg shells on the quality of the clinker and the respective cement is investigated.

2. EXPERIMENTAL

The raw materials used were limestone, sandy and fatty clays quarried from the quarries of Tourah cement plant, Suez Cement Group, Cairo, Egypt. Iron scales supplied from Alexandria Steel Company were utilized as a corrective material. Red brick powder was available from the red brick factories located in the surrounding of the cement factory and the egg shells were obtained from the alimentation market.

The oxide composition of the raw materials was determined by means of X-ray fluorescence using a Philips apparatus PW 2404 Type X-CEM. The trace elements of the red brick powder and the egg shells were detected by carrying out the scanning mode of the XRF apparatus on the samples. The alkali contents were estimated with the help of a flame photometer Jenway PFP7.

The mineralogical composition of the raw materials was defined by means of X'PERT MPD Philips X-ray diffractometer and their thermal behavior was measured by differential thermal and thermogravimetric analyses on a 60H Shimadzu equipment.

Three mixes were designed to prepare raw meals of the high belite cement with a lime saturation factor of 77%, silica and alumina modulus of ~2.2 and ~1.2 respectively (Table 1): The reference mix (M_{ref}) was prepared from 77% limestone, 11% sandy clays, 11% fatty clays and 1% iron scales. In the second mix (M_2) the fatty clays were totally replaced by 10% red brick powder and the amount of sandy clays was raised to 12%. Finally the third mix (M_3) was composed of 20% sandy clays, the fatty clays were reduced to 2% and 10% of limestone was replaced by egg shells.

The raw materials were separately dried, finely ground and sieved up to a residue of 15–17% on a 90 μ m sieve. They were intimately mixed and pressed as pellets 40 mm diameter. The pellets were burned 15 minutes in a platinum crucible at 1350 °C. At the end of the burning period the clinkers obtained were quenched in air at room temperature with an approximate cooling rate of 850 °C/minute then finely ground to a fineness <90 μ m, their free lime content indicating their burnability (30) was measured according to the method of Javellana et al. (31).

TABLE 1. Design of the raw mixes (%) and their burning parameters

	Limestone	Sandy clay	Fatty clay	Iron scales	Red brick powder	Egg shells	LSF	SM	AM
M _{1ref}	77.0	11.0	11.0	1.0%	–	–	77.10	2.22	1.26
M ₂	77.0	12.0	–	1.0%	10.0%	–	77.06	2.28	1.31
M ₃	66.7	20.3	2.0	1.0%	–	10.0%	76.61	2.24	1.23

LSF = Lime saturation factor. SM = Silica modulus AM = Alumina modulus.

The oxide composition of the clinkers was determined by means of X-ray fluorescence; (XRF, PANalytical; Model Magix Pro PW 2440, PANalytical). Their phase identification was performed with EVA software and Rietveld refinements were performed using TOPAS 3, Bruker-AXS Panalytical X'Pert. Supplementary diffractograms were obtained at low scanning modes in the 2 theta region from 25 to 35° then from 35 to 40° on the X'PERT MPD Philips X-ray diffractometer.

The boron concentration in the clinkers was checked by means of atomic absorption apparatus model GBC Avanta.

The clinkers were treated with KOH-sucrose to dissolve C₃A and C₄AF for 10 minutes (27) leaving the silicate phases (C₃S and C₂S) in the solid residues according to Gutteridge (32). The trace elements of residues were determined using the scanning mode of the X-ray fluorescence apparatus as in the case of the raw materials.

The morphology of fractured surfaces was examined with the secondary electron mode by means of Quanta 250 FEG scanning electron microscope as well as on the back scattered mode with EDAX on Zeiss EVO 50XVP, analyzer Bruker AXS XFlash Detector 410.

The gypsum content added to each clinker was estimated from the Na equivalent and C₃A in the clinker as follows: $N_{aeq} = Na\% + 0.658 K\%$, the optimum $SO_3 = 1.841 + 0.095 C_3A + 1.636 N_{aeq}$ (33). 6.9 to 7.1% of gypsum was added to the three clinkers to obtain SO₃ contents of 3.22 to 3.28%. The cements obtained were finely ground to a Blaine specific surface area of 3500 cm²/g as well as 4500 cm²/g. Their oxide and phase composition were determined as in the raw meal and their mechanical and physical properties were determined according to EN 196-1 to 6.

The compressive strength results were monitored with of a compression tester Toni Technik Model 2010.010 with an accuracy of 0.04 ± 0.01%.

3. RESULTS

3.1. Raw materials

Table 2 illustrates the percentage oxide composition of the raw materials used. The trace elements determined in the red brick powder and egg shells

shown in Table 3 indicate significant amounts of strontium (357 and 521.8 ppm), barium (388.7 and 287.1 ppm) and zirconium (375.4 and 246 ppm) in both materials respectively. The other elements are present at lower concentrations ≤ 105 ppm the samples.

The X-ray diffraction patterns of limestone indicate that the calcite phase (Cc) is the main constituent of limestone and quartz (Q) appears as a minor phase in the sample (Figure 1). In the same figure the egg shell is seen to be composed of calcite as a sole inorganic constituent.

The X-ray diffraction patterns of the clays and red brick powder are presented in Figure 2. It is clear from the figure that quartz (Q) is the main phase composing the materials. A relatively broad montmorillonite (M) hump appears in both clays beside weak to very weak patterns of feldspar (F) and kaolin (K). Other weak peaks are observed in the sandy and fatty clays probably attributed to traces from cristoballite (4.02 Å), iron aluminosilicate compounds (3.76 Å), anhydrite (3.47 Å) and illite (I). The shift in the d-values lines might be due to the broadening of the peaks as a result of their small concentrations in the samples.

The red brick powder is composed of a weak halloysite (Ha) pattern observed at 2 theta value lower than 10° beside traces of feldspar (F) and hematite (He). The weak peak appearing at 3.50 Å is attributed to the anhydrite. A clear hump is seen at a 2 theta range of 20 to 30° indicating the existence of a glassy phase in this sample.

The oxide composition of the raw mixes is given in Table 4. Their thermal behavior is illustrated in Figure 3 and show main endotherms around 700 °C in the DTA diagrams attributed to the decomposition of the calcite phase. The third mix (M₃) prepared with egg shells exhibits an additional endotherm at a lower temperature of 315 °C probably due to the decomposition of the organic constituent of this waste.

3.2. Clinkers

The results obtained from the burnability tests of the mixes are illustrated in Figure 4 and show that burning at 1350 °C leads to low free lime contents of 0.56 and 0.42% in the clinkers.

TABLE 2. Oxide composition of the raw materials (%)

Material (%)	Primary raw materials					Secondary raw materials	
	Limestone	Sandy clay	Fatty clay	Iron scales	Gypsum	Egg shells	Red brick powder
LOI	41.79	6.64	11.17	0.08	9.33	42.26	1.53
CaO	51.14	1.56	1.86	none	29.23	53.82	2.93
SiO ₂	3.63	63.51	53.98	0.27	2.54	0.06	58.75
Al ₂ O ₃	0.49	14.73	17.24	0.16	0.74	none	16.83
Fe ₂ O ₃	0.20	7.81	10.89	99.00	0.11	none	7.50
MgO	0.86	2.00	2.70	0.07	1.50	0.75	1.77
K ₂ O	0.07	1.38	1.36	none	0.09	0.07	1.22
Na ₂ O	0.10	1.36	1.27	none	0.14	0.02	1.41
SO ₃	0.37	0.03	0.16	0.17	48.41	0.98	1.47
Cl	0.13	0.05	0.05	none	0.16	0.01	0.05
TiO ₂	0.06	0.11	0.18	0.11	0.07	none	0.11
MnO	0.01	0.08	0.21	0.08	0.02	none	0.05
P ₂ O ₅	0.04	1.52	2.05	none	0.01	0.72	0.93

LOI = Loss on ignition.

TABLE 3. Trace elements of the alternative raw materials (ppm)

	V	Cr	Co	Ni	Cu	Zn	Rb	Sr	Y	Nb	Ba	Pb	Zr
Egg shells	15.7	7.6	2.7	7.4	25.3	65.8	43.3	521.8	16.6	12.4	287.1	27.2	246.3
Red brick powder	93.5	12.6	1.5	4.5	4.0	105.0	65.1	357.0	33.4	71.5	388.7	15.0	375.4

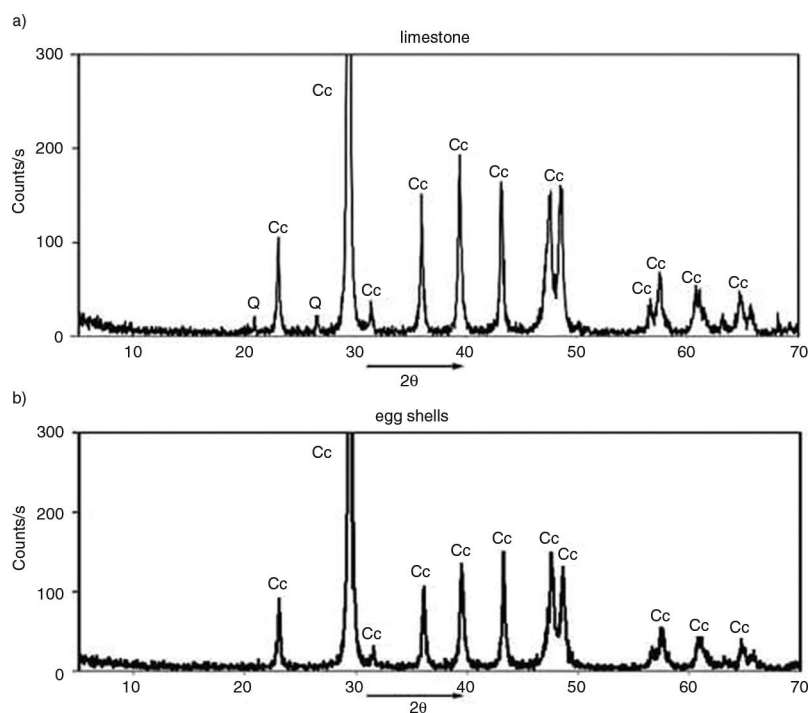


FIGURE 1. The X-ray diffraction patterns of limestone and egg shells (Cc = Calcite, Q = Quartz).

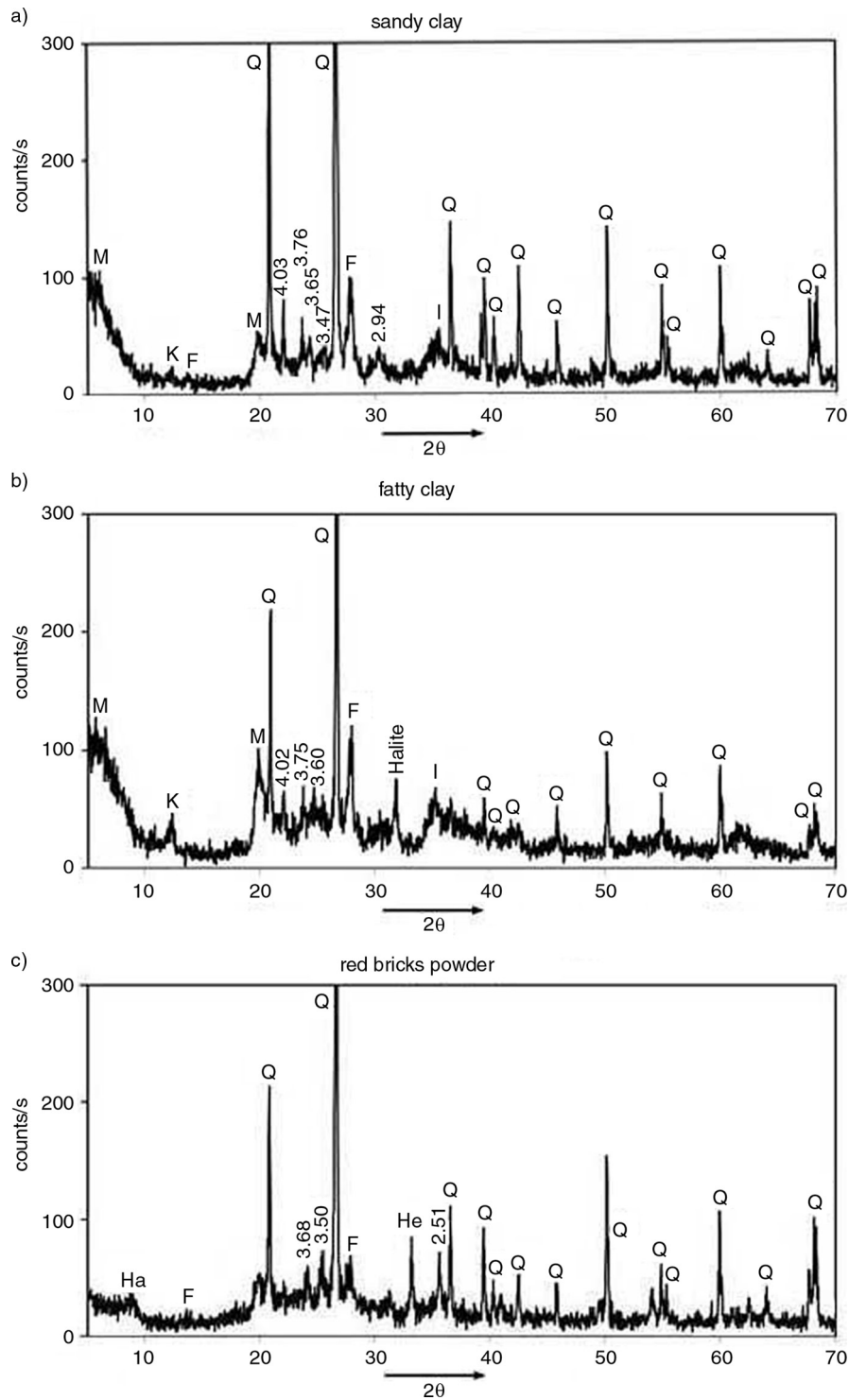


FIGURE 2. The X-ray diffraction patterns of the sandy clays, fatty clays and red brick powder (M=Montmorillonite- swelling clays, K=kaolinite, Q=Quartz, Ha=Halloysite F = Feldspar He = Hematite, I = Ilite).

The oxide composition of the clinkers is given in Table 5. Table 6 illustrates the concentration of the clinker phases as estimated from Rietveld and Bogue

equations. The predominance of the belite phase is clear from both results with acceptable deviation. The Rietveld belite values for $Clik_{1ref}$, $Clik_2$ and

TABLE 4. The oxide composition of the raw mixes (%)

	XRF											Fl. Photometer	
	L.O.I	CaO	SiO ₂	Al ₂ O ₃	Fe ₂ O ₃	MgO	SO ₃	Cl	P ₂ O ₅	MnO	TiO ₂	Na ₂ O	K ₂ O
M _{1ref}	32.96	39.43	15.74	3.96	3.14	1.39	0.30	0.27	0.43	0.06	0.10	0.35	0.31
M ₂	32.79	39.17	16.26	3.87	2.96	1.40	0.31	0.19	0.33	0.03	0.09	0.38	0.30
M ₃	34.86	39.31	15.93	3.92	3.20	1.31	0.27	0.19	0.46	0.05	0.09	0.33	0.32

Fl. photometer: Flame photometer.

Clik₃ are 64.3, 67 and 60.5% and those of Bogue are 66.9, 69.5 and 66.7% respectively. No boron could be detected in the clinker samples using the atomic absorption method of analysis.

The trace elements content of the clinker residues (after dissolution with KOH and sucrose) shows highest strontium and zirconium concentrations of 1272 and 252 ppm in Clik₂ followed by 718 and 160 ppm in Clik_{1ref} then 544 and 128 ppm in Clik₃. (Table 7). Barium is highest in Clik₃ (321 ppm), followed by Clik_{1ref} (174,8 ppm) then Clik₂ (170 ppm). The amounts of all other elements are low and lay in the range of ~32 to <2 ppm.

The electron micrographs of the reference clinker are illustrated in Figure 5 (a–c). Figure 5 (a,b) shows the microstructure of the reference sample

(Clik_{1ref}) at a secondary electron mode with few angular alite particles and several rounded belite crystals in the range of 10 μm beside interstitial phases of calcium aluminate and aluminoferrite phases. The clinker particles are submerged in a molten layer (Figure 5a). The higher magnification of Figure 5b proves the existence of clear sets of striae and twin lamellae in the belite grains and is supported by the back scattered examination of Figure 5-c.

The scanning electron micrographs of the second clinker (Clik₂) made with red brick powder indicates lower melt portion compared to Clik_{1ref} and fewer amount of the interstitial phases (Figure 6-a). No striae are observed in the high magnification picture of the secondary electron mode (Figure a–b), whereas the back scattered mode indicates weaker striation on the belite grains (Figure 5-c) compared to those of the reference clinker. Inclusions are observed in the individual grains with size lying in the range of 10 μm (Figure 5–b).

The scanning electron micrographs of the third clinker (Clik₃) prepared from egg shells and 2% from fatty clays show a lower amount of melt than in Clik_{1ref} and weak parallel striae on the rounded belite crystals (Figure 7, a-b). The morphology of the grains examined with the back scattered mode indicate a smoother surface (Figure 7-c) compared to the grains of the reference sample. Inclusions are again observed in the individual particles which maximum size is ~10 μm.

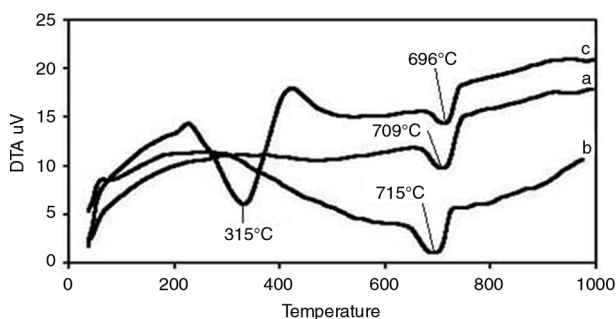


FIGURE 3. Differential thermal analysis of the three raw mixes: a) M_{1ref}, b) M₂ and c) M₃.

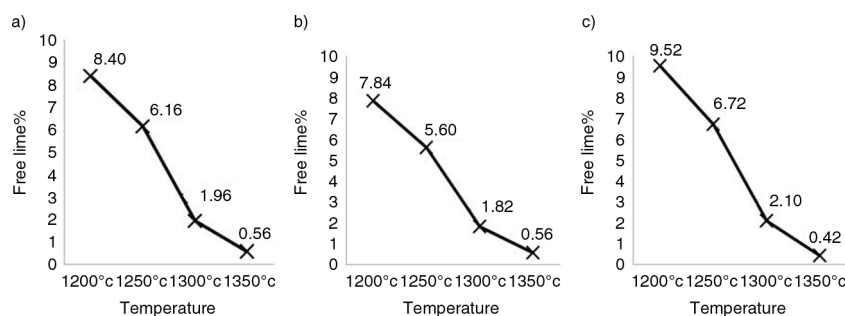


FIGURE 4. The variation in the free lime content of the raw mixes with temperature a) M_{1ref}, b) M₂, c) M₃.

TABLE 5. The oxide composition of the clinkers (%)

	XRD											Fl.photometer	
	FL	L.O.I	CaO	SiO ₂	Al ₂ O ₃	Fe ₂ O ₃	MgO	SO ₃	P ₂ O ₅	MnO	TiO ₂	Na ₂ O	K ₂ O
Clik _{1ref}	0.62	0.59	59.45	24.75	6.17	4.91	1.78	0.16	0.12	0.05	0.61	0.21	0.24
Clik ₂	0.45	0.56	59.53	25.23	5.97	4.67	1.75	0.26	0.11	0.04	0.51	0.28	0.22
Clik ₃	0.52	0.65	59.07	24.6	6.11	5.17	1.63	0.13	0.17	0.05	0.63	0.23	0.28

FL = Free lime LOI = Loss on Ignition.

TABLE 6. The phase composition of the clinkers

	C ₃ S	C ₂ S	C ₃ A cubic	C ₄ AF
Clik _{ref} (Rietveld)	5.60	64.30	11.00	13.40
Clik _{ref} (Bogue)	5.39	66.91	8.05	14.94
Clik ₂ (Rietveld)	7.70	67.10	7.20	14.30
Clik ₂ (Bogue)	3.75	69.52	7.92	14.21
Clik ₃ (Rietveld)	10.10	60.50	9.90	14.90
Clik ₃ (Bogue)	5.01	66.76	7.45	15.73

TABLE 7. Trace elements of the clinker after selective dissolution (ppm)

	V	Cr	Co	Ni	Cu	Zn	Rb	Sr	Y	Nb	Ba	Pb	Zr	La
Clik _{1ref}	23.3	16.8	7.0	5.6	<2	22.0	31.0	718.0	15.0	9.4	274.8	20.0	160	15
Clik ₂	25.5	20.3	6.4	5.6	<2	20.1	31.9	1272.0	14.3	8.4	170.0	13.0	252	16.7
Clik ₃	25.5	19.0	5.9	5.2	<2	19.5	31.7	544.5	13.6	8.3	321.0	12.7	128.7	15.8

The EDAX analysis on the three clinkers showed only the major elements in the clinkers. Element present below 0.1% could not be detected.

The X-ray diffractograms of the clinkers are illustrated in Figure 8 and prove great similarities of the patterns of the three samples and the overlap of the characteristic peaks of alite (A) with the α' and β belite modifications. The diffractograms run at a slow angle in the range of 25 to 35° allows the detection of few differences as follows:

- The main peak of the α' -belite at 2.753 Å (32.49°) is very close to that of the β -belite at 2.749 Å (32.56°) and to that of the main d-value line for alite at 2.77 Å
- A characteristic belite peak is seen at an angle of 31.04° with a d-value line of 2.81 Å
- The α' - and β -belite patterns appear in the diffractograms as a splitted peak and are relatively higher than the alite peak in Clik₃
- The characteristic patterns of C₃A identified at 2.70 Å is well recognized in Clik_{1ref}, but appears weakly in Clik₃ and is absent in Clik₂

No characteristic peaks for belite were identified in the diffractogram run in the 2 theta region of 38°.

3.3. Cements

Tables 8 and 9 show the phase composition of the three cements (Cem_{1ref}, Cem₂ and Cem₃) prepared from the clinkers studied. According to Bogue equations the C₃S content is highest in Cem₂ obtained from the red brick powder (9.99%), the belite phase amounts to 59.34%, the C₃A and C₄AF being 8.38 and 14.06% respectively. The phases composing Cem_{1ref} and Cem₃ are quite near from each other (C₃S=8.88 and 8.94%, belite=60.06 and 60.33, C₃A=7.98, 7.45 and C₄AF=14.64 and 15.31). The physical properties shown in Table 9 lay within the EN 197-1 standard specifications with respect to the consistency, setting time and soundness.

Table 10 illustrates the compressive strength of the three cements with Blaine areas of 3500 cm²/g after 3, 7, 28 and 90 days. The results obtained do not fulfill the early strength values of EN 197-1 for

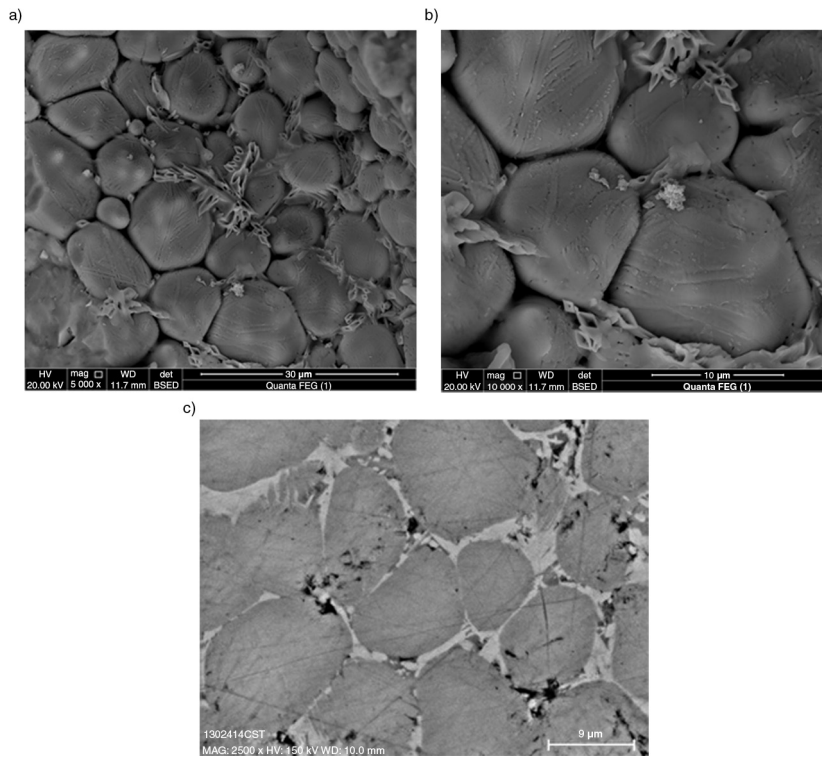


FIGURE 5. Scanning electron micrographs of the reference clinker M_{1ref} obtained from burning limestone with sandy, fatty clays and iron ores (LSF = ~77%), a and b = Secondary electron mode, c = back scattered mode.

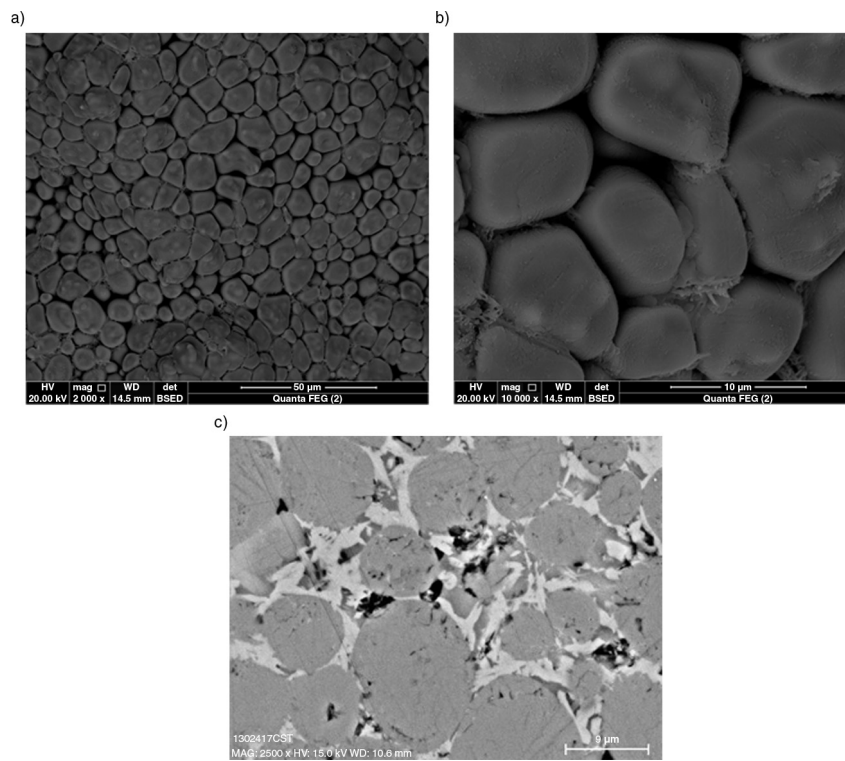


FIGURE 6. Scanning electron micrographs of Clk_2 prepared from the total replacement of fatty clays by red brick powder (LSF = ~77%), a and b = Secondary electron mode, c = back scattered mode.

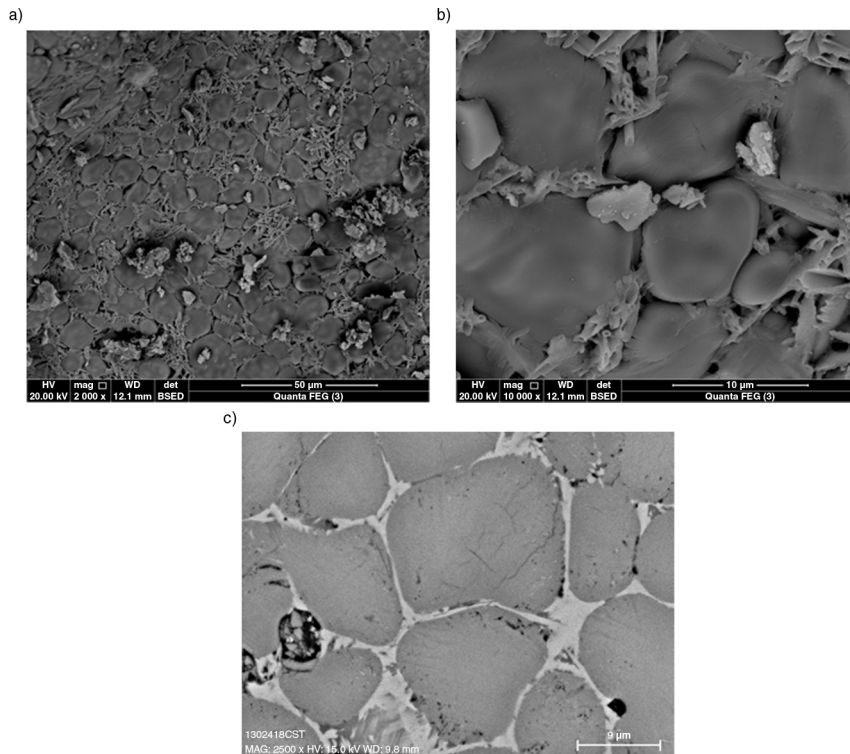


FIGURE 7. Scanning electron micrographs of Clik3 prepared from 2% of fatty clays and egg shells (LSF \approx 77%), a and b = Secondary electron mode, c = back scattered mode.

CEM I 32.5 N but satisfy the values cited for the 28 days strength as well as EN 14216 which cites strength of 22.5 and 42.5 N/mm² after 28 days without requirement for the early strength. The increase in the Blaine areas of the reference cement to 4500 cm²/g does not improve the early strength. Cem₂ exhibits the highest strength up to 90 days.

4. DISCUSSION

The manufacture of low lime cement aims to reduce the energy consumption, the green house effect as well as the production cost. It is realized through the decrease of the LSF of the clinker. Lowering the LSF from 100 to 75 leads to a 12% reduction in the theoretical heat requirement and 6% in CO₂ emission (34). The lower limit of the LSF should be higher than 75% to avoid the formation of alite-free clinker and C₁₂A₇ instead of C₃A (35).

The LSF of the clinkers produced in this work is \approx 77%. It was successfully used for the formation of high belite clinker with 60–67% C₂S, and 5–10% C₃S. The formation of the high belite clinkers is supported by the morphology of the phases in the SEM micrographs.

The differentiation between the various belite polymorphs is difficult but recent work was indicative with the use of synchrotron analysis (36–38).

The present study indicates a probable stabilization of the α' -belite polymorph in the clinkers made of alternative raw materials due to the weakness of lamina and striae in the clinker grains of Clik₂ and Clik₃.

According to the literature, the α' -belite phase is stabilized by P₂O₅ (39, 40) and concentration of up to 1.0% P₂O₅ by mass in the clinker do not have an adverse effect on its properties (40). In this work the concentrations of the phosphate in the three clinkers is below 1% and lay in the range of 0.11–0.17%. Furthermore the atomic absorption analysis proved the absence of boron, omitting thus its possible role in the formation of the α' polymorph reported in the literature (26, 38). The presence of alkali oxides with an almost equal amounts in the three clinkers; (Na₂O = 0.21–0.28%, K₂O = 0.22–0.28%) reflects its insignificant role in this phenomena. 0.1% Na₂O was reported to affect the stabilization of the active belite polymorph positively (38).

However, the significantly high concentrations of strontium (1272 ppm) in the residue of Clik₂ made of red brick powder could be a strong indication for a role played by this element in the stabilization of the α' -belite phase. Previous work was published on the strontium stabilized belite and on the α' - β transformations in strontium oxide-doped dicalcium silicate (41–43). Zirconium is the next highest concentration

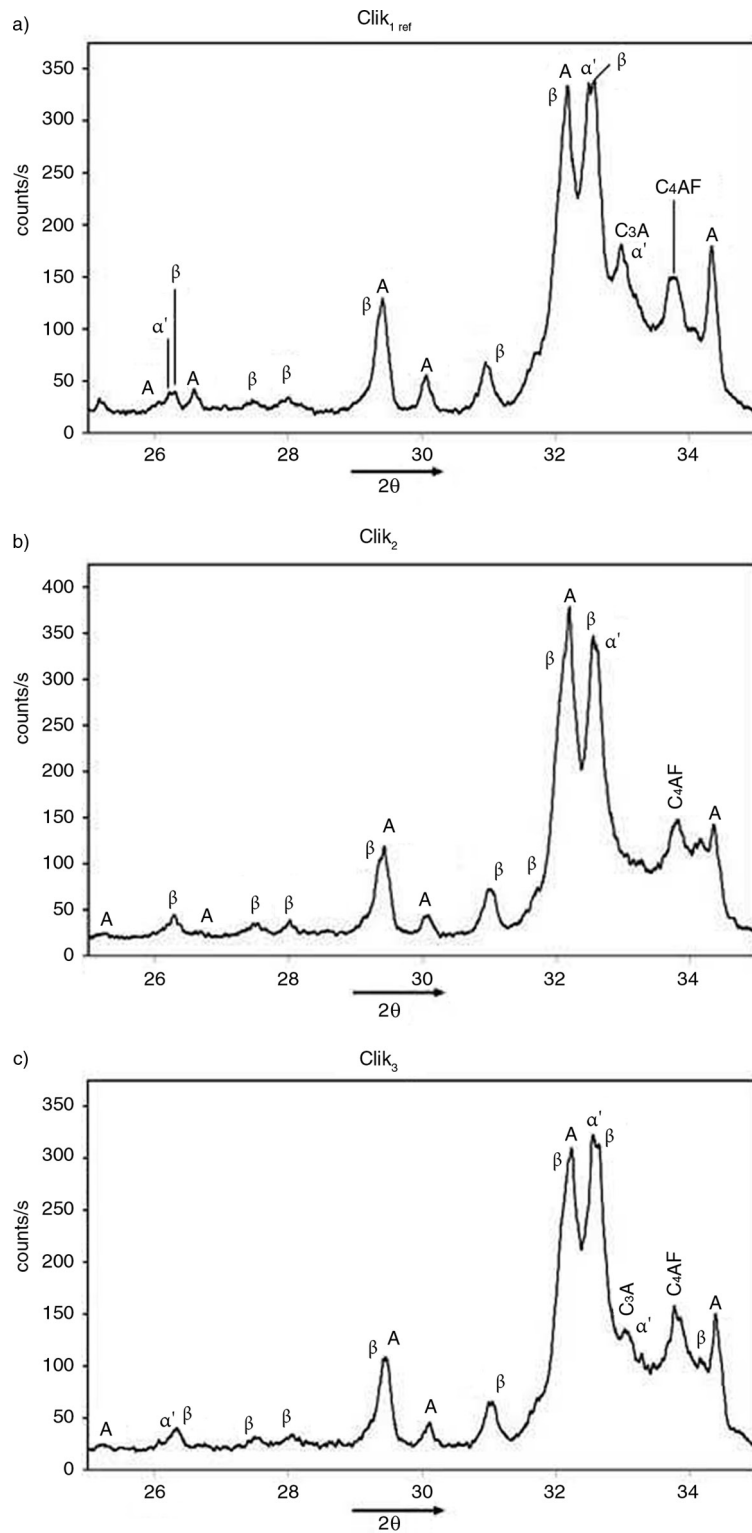


FIGURE 8. The XRD of the clinkers prepared. A = Alite, B = Belite.

in $Clík_2$ residue and amounts to 252 ppm. With reference to the literature (26, 44) a high ZrO_2 concentration does not affect the melt process.

The strontium concentration detected in $Clík_3$ made of egg shell (544.5 ppm) is lower than those of $Clík_2$ and $Clík_{1ref}$. The morphology of the clinker

TABLE 8. The oxide composition of the cements

(%)	L.O.I	CaO	SiO ₂	Al ₂ O ₃	Fe ₂ O ₃	MgO	Na ₂ O	K ₂ O	SO ₃	Cl	P ₂ O ₅	MnO	TiO ₂	IR	Naeq
Cem_{1ref}	1.37	59.67	23.26	6.08	4.81	1.85	0.26	0.24	3.32	0.035	0.63	0.10	0.16	0.92	0.42
Cem₂	1.14	59.93	23.30	6.11	4.62	1.82	0.32	0.22	3.22	0.038	0.45	0.06	0.15	0.94	0.46
Cem₃	1.20	59.84	23.37	6.02	5.03	1.72	0.23	0.28	3.28	0.037	0.67	0.07	0.13	0.90	0.41
Stand. limits	≤5								≤3.5	≤0.1				≤5	≤0.6

TABLE 9. The phase composition and physical properties of the cements

	Phase composition (%)				Physical properties			
	C ₃ S	C ₂ S	C ₃ A	C ₄ AF	Stand. Consis. (%)	I.S. (min.)	F.S. (min.)	Soundness (mm)
Cem_{1ref}	8.88	60.06	7.98	14.64	21.5	180	205	0
Cem₂	9.99	59.34	8.38	14.06	22.0	175	195	0
Cem₃	8.94	60.33	7.45	15.31	22.0	180	200	0
Stand. limits						≥75		≤10

TABLE 10. The compressive strength of the high belite cement prepared from primary and alternative raw materials

Age (d)	Compressive strength (N/mm ²)					
	Blaine 3500 cm ² /g			Blaine 4500 cm ² /g		
	Cem _{1ref}	Cem ₂	Cem ₃	Cem _{1ref}	EN 197-1	ES 4756
2	5.3	5.6	5.3	6.1		
3	6.9	7.3	7.0	7.6		
7	9.9	10.2	9.7	10.7	≥16	≥16
28	37.2	38.8	37.5	38.0	32.5–52.5	32.5–52.5
90	55.4	57.1	55.0	55.8		

grains attributed to the possible stabilization of the active belite phase could be due to the barium content (321 ppm) as previously reported in the literature (21).

The higher 28 days strength values of the second cement prepared from Clik₂ is attributed to a higher alite content but the contribution of the more reactive α' -belite modification to the strength values is not excluded.

5. CONCLUSIONS

The following conclusions can be drawn for the present work:

- Red brick powder and egg shells can be successfully used in the cement manufacture process
- The use of these secondary raw materials to replace the clays obtained from the quarry of Tourah Cement Company leads to a probable stabilization of the more reactive α' -belite
- The stabilization of the α' -belite modification could be detected by the decrease in the striation

of the belite clinker observed in the scanning electron micrograph

- A strontium concentration of 1272 ppm in the residue of red brick powder clinker and a barium content of 321 ppm in that of egg shells are expected to stabilize the active belite polymorph
- The cement made of the red brick powder clinker showed higher strength values than the other clinker

ACKNOWLEDGEMENTS

The authors would like to thank, Customer Support team, Suez Cement Group of Companies, Egypt, Italcementi Group: Mr. Stefano Gallini, Eng. M. Yildirim Manager, Eng A. Arafa and Eng. A. Abdel Moaty.

Special thanks for Eng. Xavier Guillot, R&D cement and hydraulic binders Sector Head, France, CTG, Italcementi Group. They offered us continuous support and help to achieve important analyses needed in this work.

REFERENCES

- Sleight, C. (2013) Global cement demand to see +4.9% growth. *International Construction*.
- Al Roussain, A. (2012) Opening speech. *Seventeenth Arab-International Cement Conference and Exhibition Dubai*, UAE.
- Eighth Arab Energy Conference Jordan. (2006) <http://www.elaph.com/Web/Economics/2006/5/148399.htm>.
- Intergovernmental Panel on climate change. Special report on Emissions (2001).
- McCaffrey, R. (2002) Climate change and the cement Industry. *Global Cem. Lime Mag. Environ. Spec. Issue*, 15–9.
- European Cement Industry. *Cembureau* (Organization of the Cement Industry in Europe). <http://www.cembureau.be>.
- CEMBUREAU-Environmental benefits of using alternative fuels in cement production a life cycle approach, 1998. Annual report (2001).
- EN 197-1. Cement – Part 1. (2000) Composition, specifications and uniformity criteria for common cements. *European Committee for Standardization*.
- EN 14216. Cement - Composition, specifications and conformity criteria for very low heat special cements.
- ES 4756. The Egyptian standard for cement “Composition, specifications and uniformity criteria for common cements”.
- Guerrero, A.; Goñi, S.; Campillo, I.; Moragues, A. (2004) Belite cement clinker from coal fly ash of high Ca content. Optimization of synthesis parameters. *Environ. Sci. Tech.* 38, 3209–3213. <http://dx.doi.org/10.1021/es0351589>.
- Guerrero, A.; Goñi, S.; Allegro, V.R. (2009) Durability of class C fly ash belite cement in simulated sodium chloride radioactive liquid waste: Influence of temperature. *Journal of Hazardous Materials*. 162, 1099–1102. <http://dx.doi.org/10.1016/j.jhazmat.2008.05.151>.
- Arjunam, P.; Silsbee, M.R.; Roy, D.M. (1999) Sulfaluminate - belite cement from low-calcium fly ash and sulfur-rich and other industrial by-products. *Cem. Concr. Res.* 29, 1305–1311. [http://dx.doi.org/10.1016/S0008-8846\(99\)00072-1](http://dx.doi.org/10.1016/S0008-8846(99)00072-1).
- Pimraksa, K.; Hanjitsuwan, P.; Chindaprasit, P. (2009) Synthesis of belite cement from lignite fly ash. *Ceramics International* 35, 2415–2425. <http://dx.doi.org/10.1016/j.ceramint.2009.02.006>.
- Rodrigues, F.A. (2003) Low-temperature synthesis of cements from rice hull ash. *Cem Concr Res.* 33, 1525–1529. [http://dx.doi.org/10.1016/S0008-8846\(03\)00104-2](http://dx.doi.org/10.1016/S0008-8846(03)00104-2).
- Iacobescu, R.I.; Koumpouri, D.; Pontikes, Y.; Saban, R.; Angelopoulos, G. (2011) Utilization of EAF metallurgical slag in green belite cement. *U.P.B. Sci. Bull; Series B*, 1, 73, 187–193.
- Chatterjee, A.K. (1996) High belite cements-present status and future technological opinions part 1 and 2. *Cem. Concr. Res.* 26, [8], 1213–1237. [http://dx.doi.org/10.1016/0008-8846\(96\)00099-3](http://dx.doi.org/10.1016/0008-8846(96)00099-3).
- Stark, J. (1988) Relationship between phase composition, cooling rate and Na₂O content in belite clinkers. *ZKG International* 41, [4], 169–170.
- Uchikawa, H. (1994) Management strategy in cement technology for the next century: part 3. *World cement*, 47.
- Sharp, J.H.; Lawrence, C.D.; Yang, R. (1999) Calcium sulfaluminate cements-low energy cement special cement or what? *Advance Cement Research*, 11, 3–13. <http://dx.doi.org/10.1680/adcr.1999.11.1.3>.
- Forschungsinstitut der Zementindustrie (1997) VDZ-Report 96; Verein Deutscher Zementwerke e.V.; Forschungsinstitut der Zementindustrie, Dueseldorf, 42–43.
- Viswanathan, V.N.; Raina, S. J.; Chatterjee, A.K. (1978) An exploratory investigation on Portland cement. *World Cem. Techn.* 9, [56], 109–118.
- Kuznetzonova, T.V. (1996) State of the art and prospects of special cements. 8th International Congress on the Chemistry of Cement. Rio de Janeiro 1, 283–291.
- Roppelt, T.; Dieneman, W.; Klaska, R.; Leth. I.; Sievert, Th. (2006) Use of alternative raw materials for cement clinker production. *Cement International* 1, 54–63.
- Baier, H.; Menzel, K. (2011) Utilization of alternative fuels in the cement clinker process. *Cement International* 1, 52–59.
- García-Díaz, I.; Puertas, F.; Gazulla, M.F.; Gómez, M.P.; Palacios, M. (2008) Effect of ZnO, ZrO₂ and B₂O₃ on clinkerization process. Part I. Clinkerization reactions and clinker composition. *Mater. Construcc.* 58, [292], 81–99.
- García-Díaz, I.; Puertas, F.; Gazulla, M.F.; Gomez, M. P.; Palacios, M. (2009) Effect of ZnO, ZrO₂ and B₂O₃ on clinkerization process. Part II. Phase separation and clinker phase distribution. *Mater. Construcc.* 59, [294], pp.53–74.
- Puertas, F.; García-Díaz, I.; Barba, A.; Gazulla M.F.; Palacios, M.; Gómez, M.P.; Martínez-Ramírez, S. (2008) Ceramic wastes as alternative raw materials for Portland cement clinker production. *Cem. Concr. Comp.*, 30, 798–805. <http://dx.doi.org/10.1016/j.cemconcomp.2008.06.003>.
- Lechtenberg, D. (2009) The use of alternative fuels in the cement industry of developing countries- an opportunity to reduce production costs? *Cement International*. 2, 66–70.
- Sui Tongbo.; Guo Suihua.; Liu Kezhong.; Wang Jing.; Liu Yun.; Zhao Ping.; Lu Shan.; Wang Xianbin.; Wu Zhaoqi.; (2009) Research on high belite cement. *17th Ibaasil*, Weimar Germany, 1–0025.
- Javellana, M.P.; Jawed, I. (1982) “Extraction of the free lime in Portland Cement and Clinker by Ethylene Glycol”, *Cem. Concr. Res.* 12, 309–403. [http://dx.doi.org/10.1016/0008-8846\(82\)90088-6](http://dx.doi.org/10.1016/0008-8846(82)90088-6).
- Gutteridge, W.A. (1979) On the dissolution of the interstitial phases in Portland cement. *Cem. Concr. Res.* 9, 319–324. [http://dx.doi.org/10.1016/0008-8846\(79\)90124-8](http://dx.doi.org/10.1016/0008-8846(79)90124-8).
- Holderbank, Cement Handbook, Materials technology, Volume II. (1979), pp. 16–28.
- Gygi, H. (1952) Thermodynamics of cement kiln. Proceeding of the 3rd International Symposium on the Chemistry of Cement, London, 750–79.
- Stark, J.; Mueller, A.; Schraeder, R.; Ruempler, K. (1981) Existence conditions of hydraulically active belite cement. *Zement-Kalk-Gips*, 34, 476–81.
- De la Torre, A.G.; Aranda, M.A.G.; Morsli, K.; Cuberos, A.J.M.; Zahir, M. (2007) Quantitative phase analysis of belite Portland cements from synchrotron X-ray powder diffraction. Proc. 12th International Congress on the Chemistry of Cement, Montreal, Canada. W2-06.5.
- Morsli, K.; De La Torre, A.G.; Cuberos, A.J.M.; Zahir, M.; Aranda, M.A.G. (2007) Quantitative Phase Analysis of Laboratory-Active Belite Clinkers by Synchrotron Powder Diffraction. *J. Am. Ceram. Soc.*; 90, [10], 3205–3212.
- Cuesta, A.; Losilla, E.R.; Aranda, M.A.G.; Sanz, J.; De la Torre, A.G. (2012) Reactive belite tabilization mechanisms by boron – bearing dopants. *Cem Concr Res* 42, 598–606.
- Noirfontaine, M.N.; Tusseau-Nenez, S.; Signes-Frehel, M.; Gasecki, G.; Girod-Labianca, C. (2009) Effect of phosphorous on tricalcium silicate T1: from synthesis to structural characterization. *J. Am. Cer. Soc.* 92, [10], 233–2344. <http://dx.doi.org/10.1111/j.1551-2916.2009.03092.x>.
- Punkte, S.; Schneider, M. (2008) Effect of phosphate on clinker mineralogy and cement properties. *Cement International* 6, [5], 80–93.
- Kolovos, K.; Tsivilis, S.; Kakali, G. (2005) SEM examination of clinkers containing foreign elements. *Cem. Concr. Com.* 27, 163–17. <http://dx.doi.org/10.1016/j.cemconcomp.2004.02.003>.
- Fukuda, K.; Maki, K.; Suketoshi, I. (1996) Thermal hysteresis for the α'←β transformations in strontium oxide-doped dicalcium silicates. *J. Am. Cer. Soc.* 79, [11], 2969–2970.
- Catti, M.; Gazzoni, G.; Ivaldi, G. (1984) Order-disorder in the α'-(Ca,Sr)₂SiO₄ solid solution: a structural and statistical-thermodynamic analysis, *Acta Crystallographica B*, 40, 537. <http://dx.doi.org/10.1107/S0108768184002652>.
- Kakali, G.; Kasselouri, V.; Parissakis, G. (1990) Investigation of the effect of Mo, Nb, W and Zr oxides on the formation of Portland cement clinker. *Cem. Concr. Res.* 20, 131–138. [http://dx.doi.org/10.1016/0008-8846\(90\)90123-F](http://dx.doi.org/10.1016/0008-8846(90)90123-F).